NeuroImage 224 (2021) 117413

Contents lists available at ScienceDirect

NeuroImage

journal homepage: www.elsevier.com/locate/neuroimage

Inter-individual and age-dependent variability in simulated electric fields induced by conventional transcranial electrical stimulation

Daria Antonenko[a,*], Ulrike Grittner[c,d], Guilherme Saturnino[b,e], Till Nierhaus[f], Axel Thielscher[b,e,1], Agnes Flöel[a,g,1]

[a] Department of Neurology, Universitätsmedizin Greifswald, Greifswald, Germany
[b] Danish Research Centre for Magnetic Resonance, Centre for Functional and Diagnostic Imaging and Research, Copenhagen University Hospital Hvidovre, Copenhagen, Denmark
[c] Berlin Institute of Health, Berlin, Germany
[d] Institute of Biometry and Clinical Epidemiology, Charité – Universitätsmedizin, Berlin, Germany
[e] Department of Health Technology, Technical University of Denmark, Kgs. Lyngby, Denmark
[f] Neurocomputation and Neuroimaging Unit, Department of Education and Psychology, Freie Universität Berlin, Germany
[g] German Centre for Neurodegenerative Diseases (DZNE) Standort Greifswald, Greifswald, Germany

ARTICLE INFO

Keywords:
Aging
Biophysical modelling
Non-invasive brain stimulation
Older Adults
Simulation
Transcranial direct current

ABSTRACT

Variations in head and brain anatomy determine the strength and distribution of electrical fields in humans and may account for inconsistent behavioral and neurophysiological results in transcranial electrical stimulation (tES) studies. However, it is insufficiently understood which anatomical features contribute to the variability of the modelled electric fields, and if their impact varies across age groups. In the present study, we tested the associations of global head anatomy, indexed by extra- and intra-cranial volumes, with electric field measures, comparing young and older adults. We modelled six "conventional" electrode montages typically used in tES studies using SimNIBS software in 40 individuals (20 young, 20 older adults; 20-35, 64-79 years). We extracted individual electric field strengths and focality values for each montage to identify tissue volumes that account for variability of the induced electric fields in both groups. Linear mixed models explained most of the inter-individual variability of the overall induced field strength in the brain, but not of field focality. Higher absolute head volume and relative volume of skin, skull and cerebrospinal fluid (CSF) were associated with lower overall electric field strengths. Additionally, we found interactions of age group with head volume and CSF, indicating that this relationship was mitigated in the older group. Our results demonstrate the importance to adjust brain stimulation not only according to brain atrophy, but also to additional parameters of head anatomy. Future studies need to elucidate the mechanisms underlying individual variability of tES effects in young and older adults, and verify the usefulness of the proposed models in terms of neurophysiology and behavior in empirical studies.

1. Introduction

Transcranial electrical current stimulation (tES) has been shown to alter neurotransmitter concentrations and functional activity in the brain, enhance motor and cognitive performance and augment practice gains in healthy and impaired human subjects (Dayan et al., 2013; Perceval et al., 2016; Polania et al., 2018). Due to the heterogeneity of findings, a considerable amount of research in the field of brain stimulation focuses on the exploration of factors that determine responsiveness to tES and explain interindividual variability (Krause and Cohen Kadosh, 2014; Polania et al., 2018).

Among those factors, individual variations in head and brain anatomy largely determine tES-induced current flow in the brain (Huang et al., 2017; Opitz et al., 2015). However, anatomical variations are mostly neglected in brain stimulation research with healthy participants and patients, but can be a core factor causing the variability in empirical findings (Kim et al., 2014; Laakso et al., 2015; Liu et al., 2018). Given that age-related brain atrophy affects tissue volumes in an inter-individually variable extent (Grady, 2012; Reuter-Lorenz and Park, 2014), its effects on altered current distribution induced by brain stimulation may be particularly relevant in studies with older popu-

* Corresponding author.
E-mail addresses: daria.antonenko@med.uni-greifswald.de (D. Antonenko), ulrike.grittner@charite.de (U. Grittner), guilhermebs@drcmr.dk (G. Saturnino), nierhaus@cbs.mpg.de (T. Nierhaus), axelt@drcmr.dk (A. Thielscher), agnes.floeel@med.uni-greifswald.de (A. Flöel).
[1] Contributed equally.

https://doi.org/10.1016/j.neuroimage.2020.117413
Received 23 April 2020; Received in revised form 8 September 2020; Accepted 25 September 2020
Available online 1 October 2020

lations (Antonenko et al., 2018; Mahdavi et al., 2018; Thomas et al., 2017).

The development of accessible computational modeling approaches has advanced the understanding of physical principles and neurophysiological effects of electrical current on the human brain (Hartwigsen et al., 2015; Peterchev, 2017; Thielscher et al., 2015). Several research studies have included simulation analyses for biophysical modeling of applied tES parameters in order to illustrate induced current distributions on one exemplary head model. These qualitative visualizations provide an explanatory approach to delineate the stimulated brain regions that might underlie the tES-induced physiological effects.

Modeling studies based on individualized simulation are still scarce, but essential to understand the effect of individual brain anatomy on electric field distribution. First empirical neuroscience studies have related individual model predictions to neurophysiological and behavioral tES effects (Antonenko et al., 2019; Cabral-Calderin et al., 2016; Jamil et al., 2019; Kim et al., 2014). These studies have observed associations between field strengths induced on the individual cortex by tES with cerebral blood flow (Jamil et al., 2019), with low frequency fluctuations (Cabral-Calderin et al., 2016) and with verbal working memory performance (Kim et al., 2014). In a recent study, our own group found positive relationships between electric field strengths in the sensorimotor cortex and neurochemical as well as functional connectivity modulations induced by anodal and cathodal transcranial direct current stimulation (tDCS) of the sensorimotor cortex (Antonenko et al., 2019). These studies provide evidence that predictions from electric field simulation are related to empirical findings, but most importantly, that variations in electric field distributions caused by individual head and brain anatomy contribute to inter-individual variability of physiological tES effects. However, it is so far not well understood which anatomical factors cause the observed field variations. Specifically, it is unknown how much inter-individual differences of global factors beyond age-related atrophy (see Indahlastari et al., 2020), such as head size or skull thickness, affect the model predictions, and whether these factors have a consistent impact across different montages rather than affecting current flow only for specific montages. Additionally, it is unknown if these associations vary between young and older age groups.

In the present study, we addressed these open questions by investigating the association between individual current flow estimated with computational modeling using SimNIBS software and tissue volumes derived from realistic head models using T1- and T2-weighted magnetic resonance images. We included several “conventional” electrode configurations used in tES studies in order to increase the number of observations and allow more general conclusions across montages. To address the crucial question of age effects and compare associations of the strength and focality of the tES electric field in the brain with anatomical variables, we included a young and an older age group and tested the impact of several global variables including total head volume and relative extra- and intra-cranial tissue volumes.

2. Materials and methods

2.1. Participants

Brain images of 20 young and 20 older adults were acquired. Descriptive characteristics including tissue volumes are presented in **Table 1**. The study was approved by the ethics committee of the Greifswald University Medicine and conducted in accordance with the Helsinki Declaration. Written informed consent was obtained from all participants prior to participation.

2.2. Magnetic resonance imaging

Data were acquired on a 3 T Siemens Verio equipped with a 32-channel head coil at the Baltic Imaging Center (Institute of Radiology, University Medicine Greifswald, Germany). High-resolution T1- ($1 \times 1 \times 1$ mm^3, TR = 2300 ms, TE = 2.96 ms, TI = 900 ms, flip angle = 9°; using selective water excitation for fat suppression) and T2-weighted images ($1 \times 1 \times 1$ mm^3, TR = 12770 ms, TE = 86 ms, flip angle = 111°) were recorded.

2.3. Computational modeling analysis

The software SimNIBS (version 3.0.7) was used to calculate the electric field induced by tES, based on the finite element method and individualized tetrahedral head meshes generated from the structural T1- and T2-weighted images of the participant (http://simnibs.org) (Saturnino et al., 2019; Thielscher et al., 2015; Windhoff et al., 2013). Head reconstruction was performed using the incorporated headreco tool based on SPM12 and CAT12 toolboxes (Nielsen et al., 2018). All individual datasets were visually inspected in order to assure accurate head reconstructions and tissue segmentations as suggested in (Saturnino et al., 2019). All datasets were deemed appropriate, so no manual corrections of head reconstructions were made.

Individual electroencephalography (EEG) coordinates were automatically calculated based on four fiducials (Iz, Nz, LPA, RPA) in order to obtain the 10-10 EEG positions (Jurcak et al., 2007). A plane was fitted 2 cm below the connection of Iz-Nz. The head mesh was then cut below this plane and volume of five tissue compartments (i.e., grey matter (GM), white matter, cerebrospinal fluid (CSF), skull, and skin) was extracted (please note that this was done for volume extraction only and not for e-field simulations). Head volume was calculated as sum of the volumes of all compartments. In order to obtain relative tissue volumes, absolute volumes were calculated as ratios to head volume.

2.3.1. Electric field simulation

Electric field simulations were computed for conventional bipolar tES montages with two electrodes. Anodal and cathodal electrodes were positioned based on the individual 10-10 EEG coordinates, see **Fig. 1** for electrode placements for the chosen montages. Stimulation parameters were defined as follows; two round electrodes with a 5-cm diameter, 1-1-1 mm rubber electrode layer, 3-mm gel, stimulation intensity 1 mA at anode and -1 mA at cathode. Conductivity values were set as follows; σ(white matter) = 0.126 S/m, σ(grey matter) = 0.275 S/m, σ(cerebrospinal fluid) = 1.654 S/m, s(scalp) = 0.465, σ(skull) = 0.01 S/m, σ(eye balls) = 0.500 S/m, σ(electrode rubber) = 29.4 S/m, σ(electrode gel) = 1.0 S/m.

The electric field strength and focality were extracted from the individual GM central surface output, for each tES montage. Overall induced electric field strength were indexed by the 75th percentile of the field magnitudes (for convenience, this measure is termed “general field strength” in the remainder of the paper) and focality was determined using the area of the GM region with field strengths higher than the 75th percentile. Higher values in focality represent higher spread of the current (so lower focality). To calculate average field distributions, simulation results were transformed into fsaverage space. Standard deviations were normalized to the “peak” electric field strength of the respective montage across subjects (indexed by the 99th percentile).

2.3.2. Region-of-interest (ROI) definition

We selected the following areas (regions-of-interest, ROI) from the Desikan-Killiany atlas implemented in Freesurfer (Desikan et al., 2006) in order to define intended target areas (i.e., brain region underneath the anodal electrode): left rostral middle frontal gyrus (for the montages F3-Fp2, F3-F4, and F3-P3), left precentral gyrus (for montage C3-Fp2), left inferior parietal gyrus (for montages P3-Fp2, and P3-P4). ROIs were transformed to the individual surface space and the average e-field strength was extracted.

2.4. Statistical analysis

IBM SPSS Statistics 25 (http://www-01.ibm.com/software/uk/analytics/spss/) and R (R Core Team, 2019) including the pack-

Table 1
Descriptive characteristics of the study sample.

	YNG (N=20)	OLD (N=20)	SMD	*Z*	*p*
Age in years, mean (SD)	25 (4)	70 (4)	11.0		
Sex (females), n (%)	14 (70)	14 (70)	0.0		
Total head volume (dm^3), mean (SD)	2.64 (0.26)	2.83 (0.32)	0.6	1.76	0.079
Skull volume, mean (SD)					
Absolute (dm^3)	0.42 (0.07)	0.47 (0.06)	0.7	2.19	0.028
Relative (%)	16.0 (1.6)	16.7 (2.3)	0.3	0.70	0.482
Skin volume, mean (SD)					
Absolute (dm^3)	0.76 (0.10)	0.86 (0.17)	0.7	2.11	0.035
Relative (%)	28.6 (1.6)	30.1 (3.5)	0.6	1.79	0.074
GM volume, mean (SD)					
Absolute (dm^3)	0.66 (0.05)	0.61 (0.05)	1.0	-2.76	0.006
Relative (%)	25.0 (1.5)	21.5 (1.0)	2.7	-4.95	<0.001
CSF volume, mean (SD)					
Absolute (dm^3)	0.27 (0.04)	0.39 (0.07)	2.0	4.55	<0.001
Relative (%)	10.4 (1.1)	13.7 (2.2)	1.9	4.68	<0.001
WM volume, mean (SD)					
Absolute (dm^3)	0.53 (0.06)	0.51 (0.09)	0.2	-1.15	0.250
Relative (%)	20.0 (1.2)	18.0 (1.5)	1.4	-3.57	<0.001

Total head volume and absolute tissue volumes are provided in liters/dm^3. Relative tissue volumes represent the percentage of volume in relation to total head volume. SD, standard deviation. SMD, standardized mean difference. YNG, young adults. OLD, older adults. *Z*- and *p*-values were derived from two-sided Mann-Whitney U tests.

Fig. 1. Electrode placements for the montages. Stimulation intensity in the electrodes is coded as red (1 mA) and blue (-1 mA).

ages r2glmm (Jaeger, 2017), lme4 (Bates et al., 2015), emmeans (Lenth, 2019), tableone (Yoshida, 2019) were used for statistical analysis. Linear mixed models (random intercept models) (Verbeke and Molenberghs, 2000) were calculated for each dependent variable (i.e., electric field strength and focality). Electrode montages were entered as level one units nested in different individuals as level two units (20 young adults, 20 older adults; N=40 participants / 240 data points). Models were adjusted for age group and sex. Tissue volumes (i.e., total head volume, relative volume of skin, skull, GM, and CSF) were included as covariates. In order to find the best model we first added all possible group x tissue volume interactions in a model with a total of 19 degrees of freedom and with 17 parameter estimates for the fixed effects. Subsequently, we reduced this model by dropping parameters or interactions of less importance and compared models using likelihood ratio tests and the Bayesian information criterion (BIC). The model with the smallest BIC was selected as the final model, yielding a sufficient number of parameters and avoiding overfit. Semi-partial R^2 were computed as measures of effect size for fixed effects in linear mixed model analyses (Jaeger et al., 2017). Model-based post-hoc pairwise comparisons of estimated fixed effects were computed. Subsequent linear models were computed separately for each montage and age group to explore the contribution of independent variables to average variance explanation in electric fields. Pearson's correlation coefficients were computed for linear associations between variables. The package GGally (Schloerke et al., 2018) as an extension to ggplot2 (Wickham, 2016) was used to create the correlation matrices. The reported uncorrected P-values should be interpreted within an exploratory framework, that mark tendencies and not as results of confirmatory testing of statistical hypothesis. A two-sided significance level of alpha=0.001 would be in accordance with a Bonferroni-adjusted significance level for 50 statistical tests and is used here to detect more robust statistical associations.

3. Results

As expected, older compared to young adults exhibited substantially different brain tissue volumes, such as lower volumes of grey and white matter and higher volumes of CSF, as indicated by high standardized mean difference (SMD) values (Bühner and Ziegler, 2017). Total head volumes were slightly different between groups, but this difference was not statistically significant (Z=1.76, critical value of Z: 1.96, p=0.079, 2-sided Mann-Whitney-U-test; see **Table 1**). Distribution of electric fields averaged over subjects and standard deviations are shown in **Fig. 2**, separately for each tES montage and age group. Strong fields occurred underneath the electrodes with maximum intensity between the two electrodes, consistent with previous reports (Antonenko et al., 2018; Laakso et al., 2015; Opitz et al., 2015; Polania et al., 2018; Saturnino et al., 2015). Average spatial distributions were similar between age groups with a higher variability in the young group. **Table 2** and **Fig. 3** show mean electric field strength and focality values for each montage and group.

3.1. Correlation between montages

General field strength was highly correlated between montages in both age groups, see **Fig. 4**. Correlation coefficients between focality values were rather low, with only few statistically significant correlations between montages, see **Fig. 5**.

3.2. Electric field strength and tissue volumes

Results of the linear mixed model analysis for the dependent variable general field strength are shown in **Table 3** for the Final Model (best BIC). Overall, the model identified independent variables with robust impact on general field strength across the six montages. We ob-

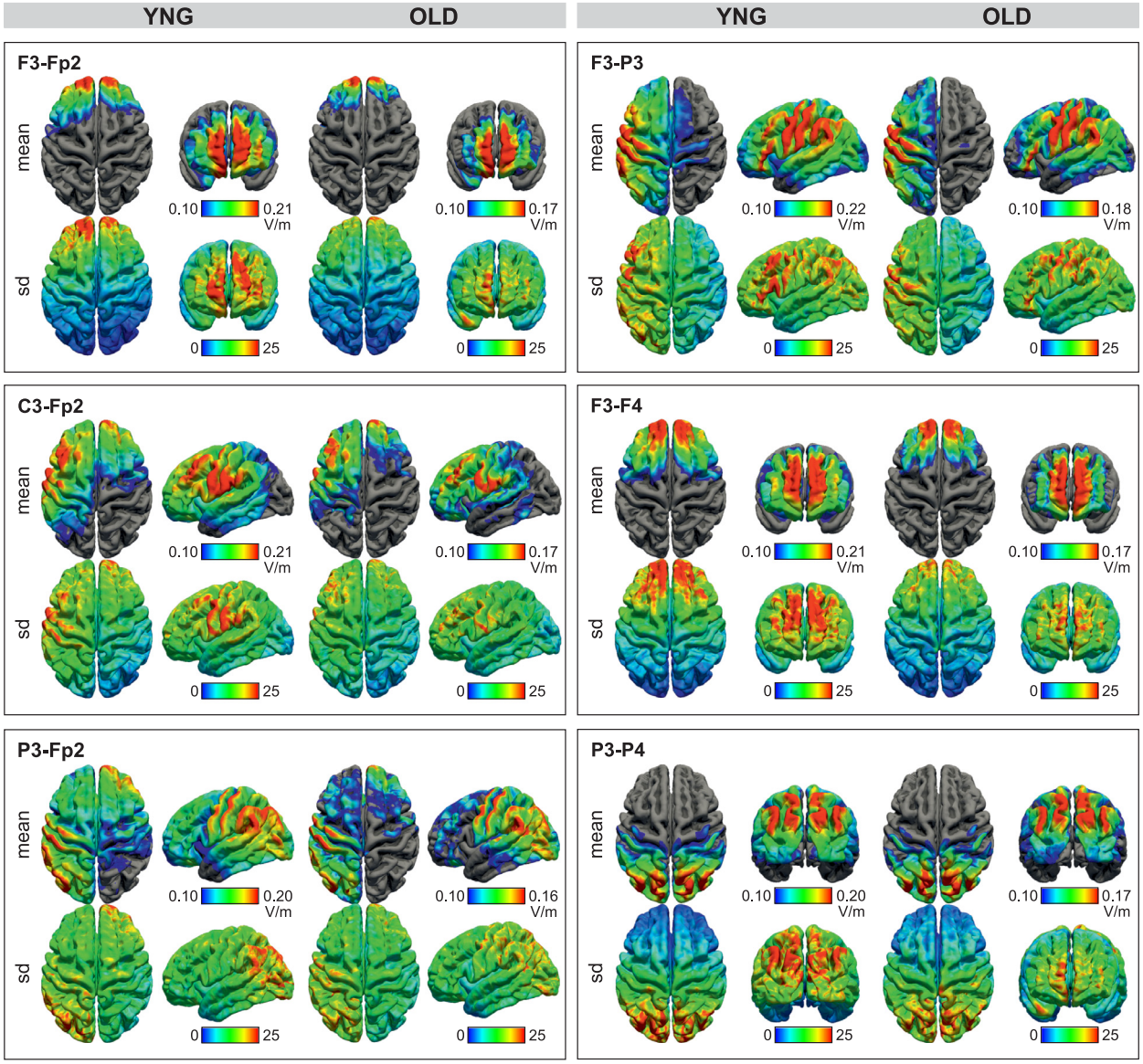

Fig. 2. Averages and standard deviations of electric field distribution for the selected montages derived from finite element method calculations using SimNIBS. Electric field strength (|E|) averages (mean; in V/m) and variability (standard deviation, SD in %) for young (YNG) and older (OLD) adults are shown. Mean images are scaled in relation to the 99th percentile of the electric field in the respective montage in each age group. SDs are scaled to the same values (99th percentile) to illustrate the percentage of variation in relation to the "peak" field strength, thus how much individual brains differed from the mean distribution. The average spatial distributions of are similar between young and older adults, with higher intensities in YNG compared to OLD. The variability in distribution of electric field strength is higher in young compared to older adults.

Table 2
General field strength and focality by group and montage.

	E-field strength (V/m)						E-field focality (10^3 mm^2)					
	F3-Fp2	C3-Fp2	P3-Fp2	F3-P3	F3-F4	P3-P4	F3-Fp2	C3-Fp2	P3-Fp2	F3-P3	F3-F4	P3-P4
YNG	0.09 (0.01)	0.14 (0.02)	0.14 (0.02)	0.13 (0.02)	0.10 (0.02)	0.11 (0.02)	3.5 (1.0)	6.1 (2.1)	9.7 (3.3)	5.4 (1.7)	4.4 (1.2)	4.3 (1.1)
OLD	0.07 (0.01)	0.11 (0.01)	0.12 (0.01)	0.11 (0.01)	0.08 (0.01)	0.10 (0.01)	3.0 (0.6)	4.8 (1.4)	6.8 (2.1)	3.4 (1.0)	3.5 (1.1)	4.4 (0.8)

Mean (SD) values are given. For n=20 in each group.

served a difference between sexes, indicating slightly higher general field strengths for males compared to females.

Older adults exhibited lower general field strength compared to young adults across montages. The Final Model revealed significant inverse associations of general field strength with total head volume, relative skull volume, relative skin volume and relative CSF volumes. Relative skin volume showed the highest effect size (semi-partial R^2=0.38), followed by relative skull (semi-partial R^2=0.30) and relative CSF volumes (semi-partial R^2=0.19). Interactions were evident between age group and total head volume and relative CSF volume, indicating that the negative association is more pronounced in young compared to older adults. For larger head volumes and more relative CSF, there is a difference in general field strength between young and older adults while this seems not to be true for smaller head volumes and lower rela-

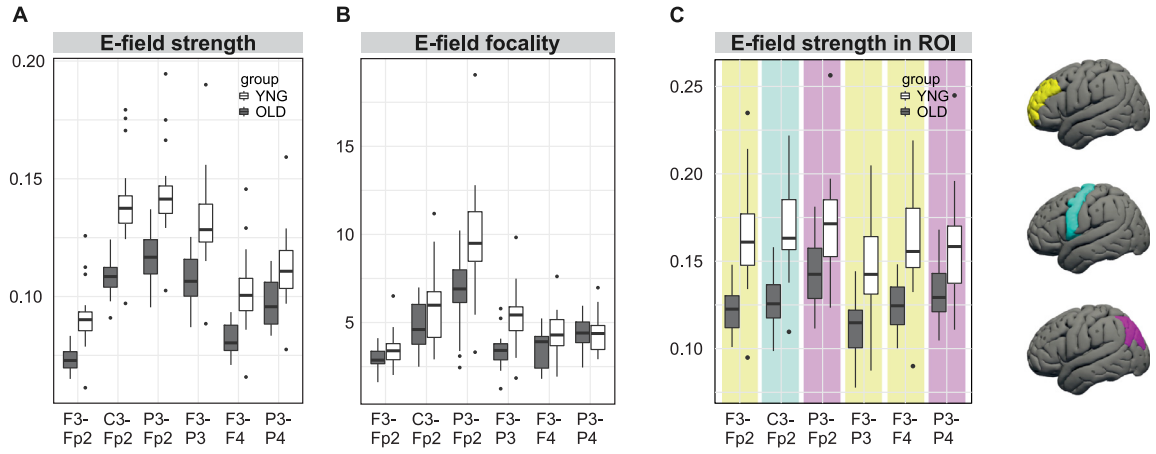

Fig. 3. Boxplots of general field strengths (in V/m, (A)), focality values (in 10^3 mm^2, (B)) and average electric field strength in regions-of-interest (ROI, (C)) by group and montage. ROI were selected from the Desikan-Killiany atlas to represent the brain area under the anodal electrode in the respective montage and are displayed on the MNI surface in the right panel (yellow: left middle frontal gyrus, cyan: left precentral gyrus, magenta: left inferior parietal gyrus). Electric field strengths, but not focality values, were lower in older compared to young adults across montages with similar patterns in both groups.

Table 3
Results of linear mixed model analyses for general field strength.

Fixed effects	E-field strength			
	beta	95%-CI	p	R^2
Intercept	0.36	0.30-0.42	<0.001	
Sex (males)	0.007	0.002-0.01	0.018	0.07
Group (YNG)	0.12	0.06-0.17	0.001	0.12
Montage (ref: C3Fp2)				
F3F4	-0.03	-0.035- -0.029	<0.001	0.67
F3Fp2	-0.04	-0.044- -0.039	<0.001	0.77
F3P3	-0.005	-0.008- -0.003	<0.001	0.05
P3Fp2	0.006	0.004-0.009	<0.001	0.07
P3P4	-0.02	-0.022- -0.017	<0.001	0.42
Total head	-0.02	-0.03- -0.01	<0.001	0.17
Skull	-0.38	-0.49- -0.27	<0.001	0.30
Skin	-0.30	-0.37- -0.23	<0.001	0.38
CSF	-0.29	-0.40- -0.18	<0.001	0.19
YNG*head	-0.01	-0.02- -0.003	0.026	0.06
YNG*skull	-0.18	-0.37- -0.01	0.101	0.03
YNG*CSF	-0.49	-0.72- -0.25	<0.001	0.13
Random effects	sigma			
subject	0.0036	0.002-0.004		
Total R^2	0.93			
BIC	-1661.1			
Log-likelihood	877.13			
df	17			

R^2, semi-partial R^2 statistic as measure of effect size. BIC, Bayesian information criterion. CI, confidence interval. YNG, young adults. Regression coefficients of linear mixed models (random intercept models) and two-sided p-values are reported.

Table 4
Results of linear mixed model analyses for focality.

Fixed effects	E-field focality			
	beta	95%-CI	p	R^2
Intercept	-9.25	-17.79- -0.71	0.050	
Sex (males)	–			
Group (yng)	0.21	-0.62-1.05	0.637	0.001
Montage (ref: C3Fp2)				
F3F4	-1.51	-2.21- -0.81	<0.001	0.07
F3Fp2	-2.22	-2.92- -1.52	<0.001	0.15
F3P3	-1.09	-1.79- -0.39	0.003	0.10
P3Fp2	2.81	2.11-3.51	<0.001	0.22
P3P4	-1.08	-1.78- -0.38	0.003	0.04
Total head vol	0.93	-0.01-1.87	0.071	0.02
Skull vol	–			
Skin vol	10.14	0.03-20.25	0.068	0.02
GM vol	39.00	14.50-63.50	0.005	0.05
Random effects	sigma			
subject	0.30	0.00-0.57		
Total R^2	0.57			
BIC	973.52			
Log-likelihood	-453.88			
df	12			

R^2, semi-partial R^2 statistic as measure of effect size. BIC, Bayesian information criterion. CI, confidence interval. Yng, young adults. Regression coefficients of linear mixed models (random intercept models) and two-sided p-values are reported.

tive CSF. The largest group difference for the association with general field strength was found for relative CSF volume (semi-partial R^2=0.13, Fig. 6).

Subsequent explorative linear models revealed that across montages, anatomical variables alone could account for 79-94 % of inter-individual variance in the general field strength (**Supplementary Tab. S1**). This effect seemed to be more pronounced in the young group, where the variables explained 75-93 % of variance in general field strength. In older adults, variance explanation ranged between 49-84 % across montages.

To analyze how much variance was explained by age, we calculated a model with age group as the only independent variable. Age group accounted for 23 % (95 %-CI: [14, 33 %]) of the variance in general field strength. After accounting for other covariates (full model), the age group still explained 12 % of total variance in general field strength (according to the semi-partial R^2-value, Edwards et al., 2008).

Linear mixed model analysis using absolute instead of relative tissue volumes showed similar results (**Supplementary Table S2**). Likewise, results were similar for other cutoff values of general field strength (see **Supplementary Table S3** for the 90th percentile, **Supplementary Table S4** for the median). For the average electric field strengths in the ROIs, the Final Model revealed similar results as for the global measures (median/50th, 75th, and 90th percentiles): Increased head, skull, skin and CSF volumes were associated with lower average e-field strength. Group*Volume interactions were observed for skull and CSF, but not for head (**Supplementary Table S5**).

3.3. Focality and tissue volumes

As a complementary parameter for quantification of the electric field distributions in the brain, focality values were explored. Results of the linear mixed model analysis for the dependent variable electric field focality are shown in Table 4 for the Final Model (best BIC). The Final

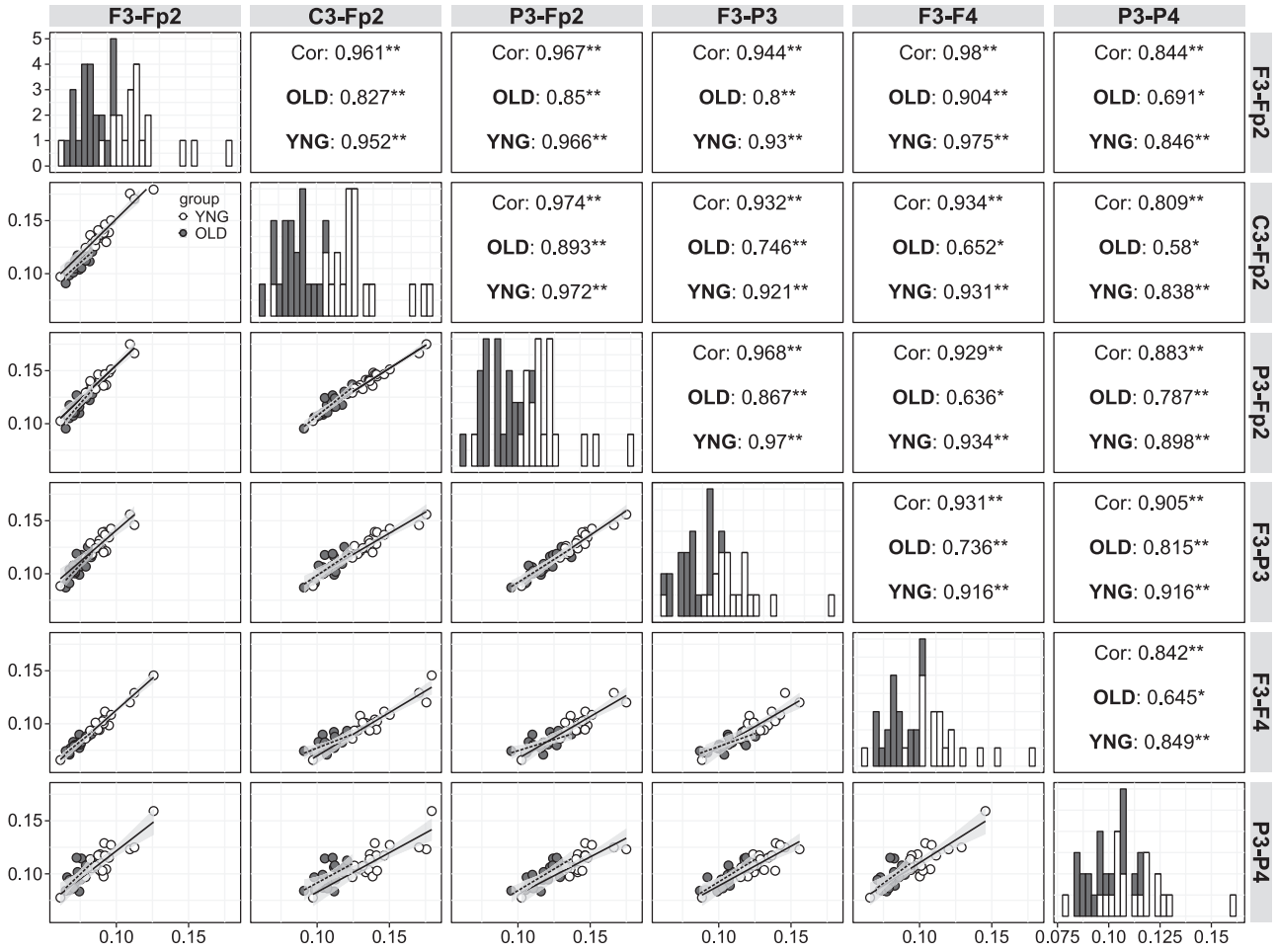

Fig. 4. Correlations of general field strengths (in V/m) between montages. Blank circles, young (YNG). Filled circles, older adults (OLD). General field strength was highly correlated between montages in both age groups. * Correlation is significant at the 0.01 level (2-tailed). ** Correlation is significant at the 0.001 level (2-tailed).

Model revealed a significant positive association of focality with relative GM volume, indicating more focal stimulation with less relative GM volume in both age groups. No other main effect was significant. No interaction remained in the Final Model.

Linear mixed model analysis using absolute instead of relative tissue volumes (**Supplementary Table S6**) and for another cutoff of focality (see **Supplementary Table S7** for the median) showed similar results.

4. Discussion

In this computational modeling study, we investigated the relationship between electric field strengths and focality induced by conventional tES electrode montages in young and older adults with tissue volumes of the head, including total head volume and relative skin, skull, and intra-cranial volumes, using linear mixed model analyses. General field strength, but not focality, was highly correlated across montages. We found a robust inverse relationship between general field strength and absolute head volume, relative skull, skin, and CSF volumes. In addition, we observed an interaction between age group and relative CSF volumes, indicating stronger linear associations in young compared to older adults.

4.1. Electric field distributions across groups

Distributions of electric fields were highly similar between age groups. Both groups exhibited rather high inter-individual variability of up to 25 % with regard to field peaks (i.e., the 99th percentiles). This is consistent with previous reports of group-wise modeling studies (Antonenko et al., 2019; Laakso et al., 2015; Mikkonen et al., 2020; Muffel et al., 2019). Importantly, this finding argues in favor of individualized modeling based on head models from an appropriate cohort (including multiple subjects of e.g. similar age), instead of using single-head models to draw conclusions about field differences between groups (Indahlastari et al., 2020).

4.2. Electric field associations across montages

Inter-individual variations of the general field strengths were highly consistent between the simulated two-channel bilateral montages in both age groups, and a substantial amount of the inter-individual variability of the general field strengths could be explained by variations of rather general anatomical factors such as total head or CSF volume. Interestingly, this shows that more complex anatomical features such as differences in the gyrification pattern contribute only little to the observed individual variations in the overall induced field strengths, at least for the unfocal montages tested here. When assuming that the physiological effects of tES have a similar dependence on e-field strength across different brain regions, our results suggest that also the inter-individual variability of the physiological and behavioral stimulation effects might to some extent be consistent across montages. Clearly, this hypothesis needs to be addressed in future empirical tES studies.

Associations between field focality values across montages were rather low, probably indicating that specific factors such as regional

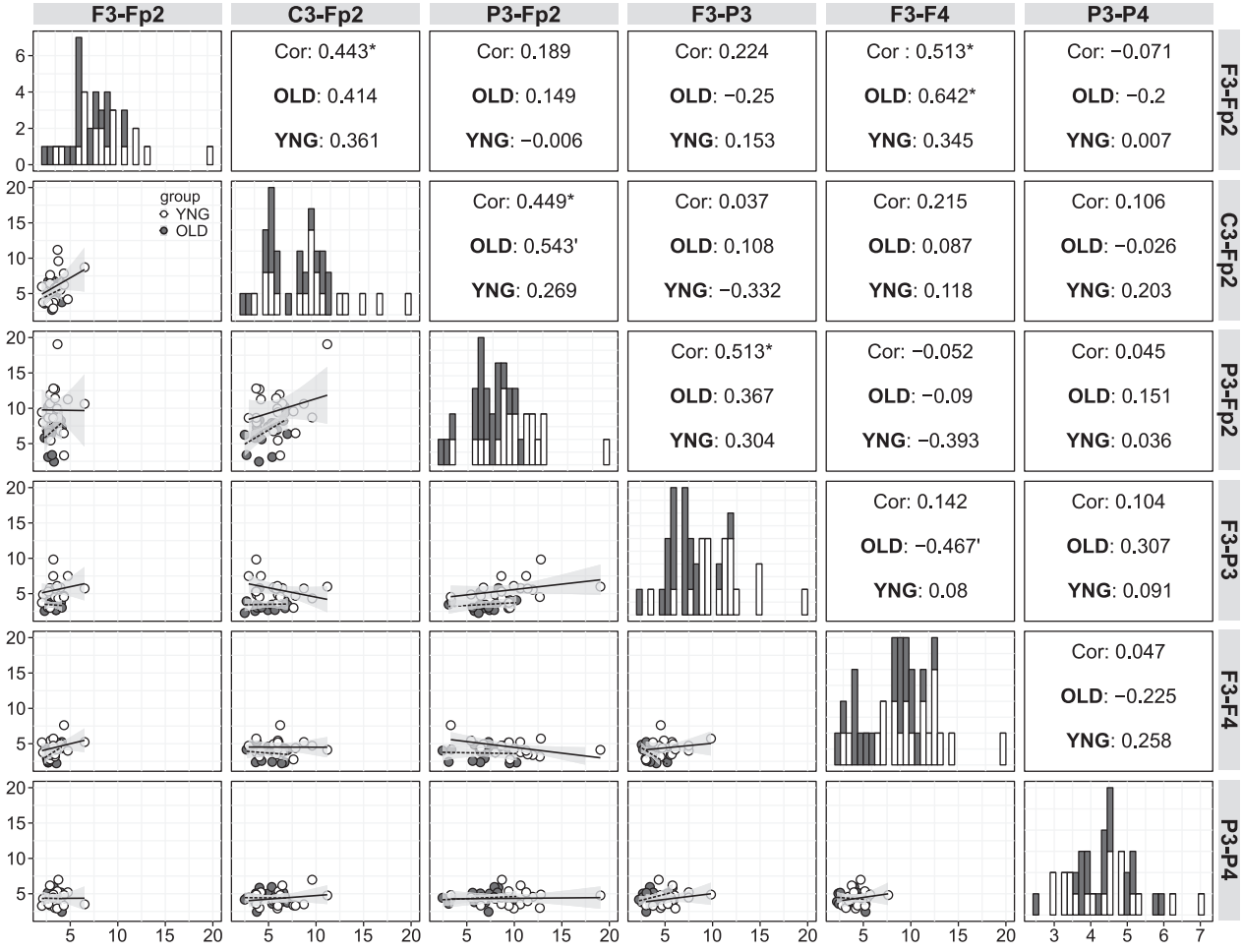

Fig. 5. Correlations of focality (in 10^3 mm^2) between montages. Blank circles, young (YNG). Filled circles, older adults (OLD). Higher values represent lower focality. Correlation is significant at the 0.05 level (2-tailed). Focality was overall not correlated between montages in both age groups. * Correlation is significant at the 0.01 level (2-tailed). No correlation remained significant at the 0.001 level (2-tailed).

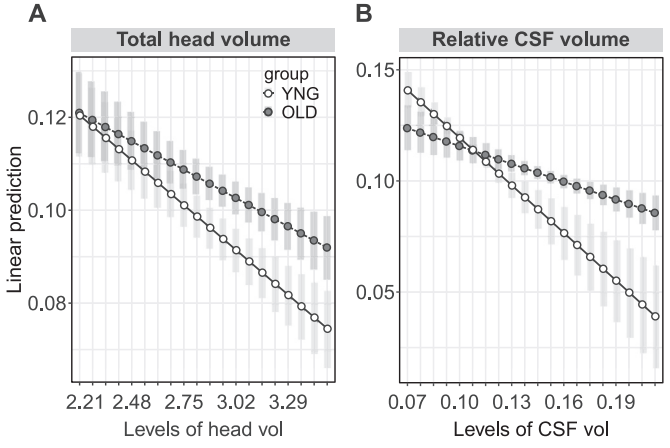

Fig. 6. Visualization of interaction effects in the final model for general field strength. Young adults exhibited steeper inverse associations of general field strength with head (A) and CSF volume (B).

extra- or intra-cranial volumes and cortical folding patterns may contribute to the spatial distribution induced by each electrode configuration. It is yet unclear how those parameters impact empirical tES effects, i.e., both neurophysiological and behavioral parameters, an issue to be elucidated in future studies.

4.3. Age-associated change in electric field strengths and its association with anatomical variables

Previous studies have observed lower field peaks with increased age (Antonenko et al., 2018; Laakso et al., 2015; Mahdavi et al., 2018; Muffel et al., 2019). Two studies have evaluated the impact of brain shrinkage due to aging and cognitive impairment (Thomas et al. 2018; Mahdavi et al. 2018) on current flow. The results showed reduced current density in a brain of an older (cognitively impaired) individual compared to a brain of a young individual (Mahdavi et al. 2018). Investigating electric field variability in 5 individuals with an age range of 43 to 85 years did not show a clear linear association with CSF volume (Thomas et al. 2017). These first studies have provided important preliminary evidence for the role of brain atrophy in determining electric fields. However, head models were based only on a few individual brains with no information about absolute or relative tissue volumes. Our study confirmed these findings, given that the comparison of general field strength between age groups showed lower values in older compared to young adults. The first modeling study that included a large group of older adults demonstrated an association between higher age-related brain atrophy with lower induced current field density (Indahlastari et al., 2020). The authors used individualized head models of older adults, ranging from 50 to 95 years, to simulate current fields in two electrode montages (i.e., primary-motor and prefrontal), and relate local brain regional field measures to brain atrophy, age and brain-to-CSF ratios. Interestingly, the association of age and current den-

sity was mediated by each individual's ratio between brain (i.e., GM and WM volumes) and CSF. Our findings are in line with this recent report, confirming the impact of relative CSF volume on tES-induced field strength in the brain (Laakso et al., 2015; Mikkonen et al., 2020; Opitz et al., 2015). We extend the results of Indahlastari et al. by additionally comparing this relationship in older adults to the relationship in a young group, and including not only intra- but also extra-cranial volume measures. Of note, as Indahlastari et al. (2020) assessed an average current dose across gray and white matter, the confirmation of a dose difference-atrophy relationship in GM is important because tES is thought to affect only GM. In addition, we were able to demonstrate that brain atrophy is only one of several anatomical features with relevance for the induced field strength. In particular, our study reveals that inter-individual variations in total head volumes, including extra-cranial tissue volumes in skull and skin, contribute to a similar extent to the variability of the electric field in brain GM as intra-cranial volumes (e.g., CSF). In contrast to some of the previous approaches that used ROI analyses (Mikkonen et al., 2020; Opitz et al., 2015), we demonstrated a clear association between field strength and tissue volumes of the whole head and brain. In order to be able to draw conclusions independent of a specific electrode configuration, we included six conventional montages (Muffel et al., 2019). Most of the previous modeling studies (Indahlastari et al., 2020; Laakso et al., 2015; Opitz et al., 2015) used only tES over primary-motor and/or frontal brain areas, so it had remained elusive whether their findings were specific to those montages.

Volume of CSF, together with volume of skin, skull, and total head explained 79-94 % of variability, thus constituting the main determinants of general field strength. Higher tissue volumes were related to lower strengths of the e-field with highest effect sizes for skull and skin, followed by CSF and total head volume. These effects were seen across age groups and montages. Further exploratory analyses showed that the amount of variance these anatomical variables explained was higher in young adults. In addition, our observation of an interaction between age group and CSF volumes is indicative of a lower impact of CSF volumes on general field strength in older adults. Speculatively, as higher CSF volumes in older adults increase the amount of current flow in CSF, this effect might also increase the impact of inter-individual anatomical variations of sulcal shape on the current flow patterns. This, in turn, would decrease the relevance of the general anatomical features tested here. Alternatively, this finding might point towards a non-linear relationship between age-related atrophy and tES-induced e-field strengths. In sum, our data show that age-related atrophy (i.e., relative CSF volume) as well as head anatomy (i.e., total head volume, and relative skull and skin volumes) impact tES-induced field strengths.

4.4. Complementary analyses of electric field focality

Complementary to electric field strength, we employed a focality metric as index of the spatial extent of the induced field. Young adults showed a tendency towards a lower focality compared to older adults in some of the montages. This finding might have been due to higher relative GM volumes in young adults that resulted in less focal tES effects. Focality is generally low for the simulated conventional bipolar montages, and we have little knowledge whether size variations of these extended fields could be expected to influence the physiological tES effects. We may speculate that the more widely spread areas of high field strengths in young adults might ensure a more robust stimulation of the target areas and thus help to reduce the variability of the physiological effects compared to older adults. However, this hypothesis will have to be followed up in empirical studies.

4.5. Strengths and limitations

Several limitations should be considered when interpreting our findings. First, we derived conclusions from modeling data only. As we did not include empirical data, we are not able to draw conclusions about the functional significance of the inter-individual variability of general field strength and focality. Whether or not they impact behavioral or neurophysiological response in young and older adults has to be investigated in future studies. Importantly, in addition to anatomy, brain state has been recognized to interact with tES effects and should be considered together with simulation results (Esmaeilpour et al., 2019). Our computational modeling study now provides the starting point for these empirical studies. Second, in our sample, young and older adults exhibited differences in tissue volumes that can be partly attributed to age (e.g., in case of intra-cranial volume differences), but may also be cohort-specific (e.g., in case of extra-cranial volume differences). This factor should be kept in mind when drawing conclusions about the specific contribution of age to electric fields. However, differences were not pronounced and our statistical models accounted for them. Third, the segmentation and simulation method strongly influence the results of computational modeling studies (Nielsen et al., 2018; Puonti et al., 2019). It is conceivable that different methods lead to different results (Puonti et al., 2019). Importantly, in addition to group-wise individual modeling, we encourage future investigations to include T2w images which improve the segmentation of the CSF-skull boundary and ensure that the skull compartment is reconstructed with good accuracy when used within the head modeling approach employed here (Nielsen et al., 2018; Puonti et al., 2019). Fourth, modeling approaches in general depend on conductivity values which – in the simulation – are assumed to be constant between all individuals in the simulation. However, there is some data available on age-related conductivity changes of the skull, caused by calcification changes (Hoekema et al., 2003; McCann et al., 2019). On the other hand, the conductivity of CSF seems to be relatively stable across the age range (Baumann et al., 1997) and only little affected by the changes in protein concentration reported in Garton et al. (1991). Available data on this topic is so far very sparse and conductivity change might be a further factor that contributes to systematic differences between the fields between young and older adults (McCann et al., 2019). In general, we would expect that lower skull conductivity increases the amount of current shunted through the skin and thus decreases the peak fields observed in older participants even further. We have no systematic knowledge about age-related conductivity changes of other tissue compartments, indicating that future work should validate the assumed conductivities across the age range to ensure robustness of individual field predictions. Fifth, we used a limited set of parameters, including only round electrodes and conventional tES montages, and only extracted norm components of the electric field (i.e., the strength of the electric field, irrespective of its direction). Previous work has shown almost no effect of electrode form (Mikkonen et al., 2020), but it is feasible that other montages such as more focal high-density electrode configurations or other components of the field (such as normal components, including information about directionality of the field) will show different relationships with anatomical features.

5. Conclusion

In conclusion, in the present computational modeling study, we showed that (a) the induced electric fields differed between age groups, (b) head, skull and skin volumes impact the overall electric field strength to a similar extent as CSF volume, and (c) the impact of CSF volumes is lower in older compared to young adults. The anatomical variables included in our model explained most of the variability of the general field strength in the brain, and should therefore be considered when calculating specific electric fields for empirical tES studies. Our results advance the understanding of individual variability of tES effects in young and older adults and help promote precision brain stimulation techniques.

Declaration of Competing Interest

None.

Credit authorship contribution statement

Daria Antonenko: Conceptualization, Formal analysis, Investigation, Writing - original draft, Writing - review & editing, Visualization, Project administration, Funding acquisition. **Ulrike Grittner:** Formal analysis, Visualization. **Guilherme Saturnino:** Software, Formal analysis. **Till Nierhaus:** Software, Formal analysis. **Axel Thielscher:** Conceptualization, Writing - original draft, Writing - review & editing, Funding acquisition. **Agnes Flöel:** Writing - original draft, Writing - review & editing, Supervision, Funding acquisition.

Funding

This work was supported by the Bundesministerium für Bildung und Forschung (grant number 01GQ1424A to AF); the Deutsche Forschungsgemeinschaft (grant numbers FL 379/24-1, 327654276 – SFB 1315 to AF, AN 1103/3-1 to DA); the Lundbeck foundation (grant numbers R244-2017-196, R186-2015-2138 to AT); and the Novonordisk foundation (grant number NNF14OC0011413 to AT, with principal investigator Hartwig Siebner).

Supplementary materials

Supplementary material associated with this article can be found, in the online version, at doi:10.1016/j.neuroimage.2020.117413.

References

Antonenko, D., Nierhaus, T., Meinzer, M., Prehn, K., Thielscher, A., Ittermann, B., Floel, A., 2018. Age-dependent effects of brain stimulation on network centrality. Neuroimage 176, 71–82.

Antonenko, D., Thielscher, A., Saturnino, G.B., Aydin, S., Ittermann, B., Grittner, U., Flöel, A., 2019. Towards precise brain stimulation: Is electric field simulation related to neuromodulation? Brain Stimul. 12, 1159–1168.

Bates, D., Maechler, M., Bolker, B., Walker, S., 2015. Fitting linear mixed-effects models using lme4. J. Stat. Softw. 67, 1–48.

Baumann, S.B., Wozny, D.R., Kelly, S.K., Meno, F.M., 1997. The electrical conductivity of human cerebrospinal fluid at body temperature. IEEE Trans. Biomed. Eng. 44, 220–223.

Bühner, M., Ziegler, M., 2017. Statistik für Psychologen und Sozialwissenschaftler [statistics for psychologists and social scientists]. Pearson, Munich.

Cabral-Calderin, Y., Williams, K.A., Opitz, A., Dechent, P., Wilke, M., 2016. Transcranial alternating current stimulation modulates spontaneous low frequency fluctuations as measured with fMRI. Neuroimage 141, 88–107.

Dayan, E., Censor, N., Buch, E.R., Sandrini, M., Cohen, L.G., 2013. Noninvasive brain stimulation: from physiology to network dynamics and back. Nat. Neurosci. 16, 838.

Desikan, R.S., Segonne, F., Fischl, B., Quinn, B.T., Dickerson, B.C., Blacker, D., Buckner, R.L., Dale, A.M., Maguire, R.P., Hyman, B.T., Albert, M.S., Killiany, R.J., 2006. An automated labeling system for subdividing the human cerebral cortex on MRI scans into gyral based regions of interest. Neuroimage 31, 968–980.

Edwards, L.J., Muller, K.E., Wolfinger, R.D., Qaqish, B.F., Schabenberger, O., 2008. An R2 statistic for fixed effects in the linear mixed model. Stat Med 27, 6137–6157.

Esmaeilpour, Z., Shereen, A.D., Ghobadi-Azbari, P., Datta, A., Woods, A.J., Ironside, M., O'Shea, J., Kirk, U., Bikson, M., Ekhtiari, H., 2019. Methodology for tDCS integration with fMRI. Hum. Brain Mapp..

Garton, M.J., Keir, G., Lakshmi, M.V., Thompson, E.J., 1991. Age-related changes in cerebrospinal fluid protein concentrations. J. Neurol. Sci. 104, 74–80.

Grady, C., 2012. The cognitive neuroscience of ageing. Nat. Rev. Neurosci. 13, 491–505.

Hartwigsen, G., Bergmann, T.O., Herz, D.M., Angstmann, S., Karabanov, A., Raffin, E., Thielscher, A., Siebner, H.R., 2015. Modeling the effects of noninvasive transcranial brain stimulation at the biophysical, network, and cognitive level. Prog. Brain Res. 222, 261–287.

Hoekema, R., Wieneke, G.H., Leijten, F.S., van Veelen, C.W., van Rijen, P.C., Huiskamp, G.J., Ansems, J., van Huffelen, A.C., 2003. Measurement of the conductivity of skull, temporarily removed during epilepsy surgery. Brain Topogr. 16, 29–38.

Huang, Y., Liu, A.A., Lafon, B., Friedman, D., Dayan, M., Wang, X., Bikson, M., Doyle, W.K., Devinsky, O., Parra, L.C., 2017. Measurements and models of electric fields in the in vivo human brain during transcranial electric stimulation. eLife 6, e18834.

Indahlastari, A., Albizu, A., O'Shea, A., Forbes, M.A., Nissim, N.R., Kraft, J.N., Evangelista, N.D., Hausman, H.K., Woods, A.J., 2020. Modeling transcranial electrical stimulation in the aging brain. Brain Stimul. 13, 664–674.

Jaeger, B.C., 2017. r2glmm: Computes R Squared for Mixed (Multilevel) Models R package version 0.1.2. https://CRAN.R-project.org/package=r2glmm.

Jaeger, B.C., Edwards, L.J., Das, K., Sen, P.K., 2017. An R2 statistic for fixed effects in the generalized linear mixed model. J. Appl. Stat. 44, 1086–1105.

Jamil, A., Batsikadze, G., Kuo, H.-I., Meesen, R.L.J., Dechent, P., Paulus, W., Nitsche, M.A., 2019. Current intensity- and polarity-specific online and aftereffects of transcranial direct current stimulation: An fMRI study. Hum. Brain Mapp. n/a.

Jurcak, V., Tsuzuki, D., Dan, I., 2007. 10/20, 10/10, and 10/5 systems revisited: their validity as relative head-surface-based positioning systems. Neuroimage 34, 1600–1611.

Kim, J.H., Kim, D.W., Chang, W.H., Kim, Y.H., Kim, K., Im, C.H., 2014. Inconsistent outcomes of transcranial direct current stimulation may originate from anatomical differences among individuals: electric field simulation using individual MRI data. Neurosci Lett 564, 6–10.

Krause, B., Cohen Kadosh, R., 2014. Not all brains are created equal: the relevance of individual differences in responsiveness to transcranial electrical stimulation. Front Syst Neurosci 8, 25.

Laakso, I., Tanaka, S., Koyama, S., De Santis, V., Hirata, A., 2015. Inter-subject Variability in Electric Fields of Motor Cortical tDCS. Brain Stimul 8, 906–913.

Lenth, R., 2019. emmeans: Estimated Marginal Means, aka Least-Squares Means. R package version 1.4.3.01. https://CRAN.R-project.org/package=emmeans.

Liu, A., Vöröslakos, M., Kronberg, G., Henin, S., Krause, M.R., Huang, Y., Opitz, A., Mehta, A., Pack, C.C., Krekelberg, B., Berényi, A., Parra, L.C., Melloni, L., Devinsky, O., Buzsáki, G., 2018. Immediate neurophysiological effects of transcranial electrical stimulation. Nat. Commun. 9, 5092.

Mahdavi, S., Towhidkhah, F., Alzheimer's Disease Neuroimaging, I., 2018. Computational human head models of tDCS: Influence of brain atrophy on current density distribution. Brain Stimul. 11, 104–107.

McCann, H., Pisano, G., Beltrachini, L., 2019. Variation in reported human head tissue electrical conductivity values. Brain Topogr. 32, 825–858.

Mikkonen, M., Laakso, I., Tanaka, S., Hirata, A., 2020. Cost of focality in TDCS: Interindividual variability in electric fields. Brain Stimul. 13, 117–124.

Muffel, T., Kirsch, F., Shih, P.-C., Kalloch, B., Schaumberg, S., Villringer, A., Sehm, B., 2019. Anodal transcranial direct current stimulation over S1 differentially modulates proprioceptive accuracy in young and old adults. Front. Aging Neurosci. 11.

Nielsen, J.D., Madsen, K.H., Puonti, O., Siebner, H.R., Bauer, C., Madsen, C.G., Saturnino, G.B., Thielscher, A., 2018. Automatic skull segmentation from MR images for realistic volume conductor models of the head: Assessment of the state-of-the-art. Neuroimage 174, 587–598.

Opitz, A., Paulus, W., Will, S., Antunes, A., Thielscher, A., 2015. Determinants of the electric field during transcranial direct current stimulation. Neuroimage 109, 140–150.

Perceval, G., Flöel, A., Meinzer, M., 2016. Can transcranial direct current stimulation counteract age-associated functional impairment? Neurosci. Biobehav. Rev. 65, 157–172.

Peterchev, A.V., 2017. Transcranial electric stimulation seen from within the brain. eLife 6, e25812.

Polania, R., Nitsche, M.A., Ruff, C.C., 2018. Studying and modifying brain function with non-invasive brain stimulation. Nat. Neurosci. 21, 174–187.

Puonti, O., Saturnino, G.B., Madsen, K.H., Thielscher, A., 2019. Value and limitations of intracranial recordings for validating electric field modeling for transcranial brain stimulation. Neuroimage 208, 116431.

Core Team, R, 2019. R: A language and environment for statistical computing. R Foundation for Statistical Computing Vienna, Austria. URL https://www.R-project.org/.

Reuter-Lorenz, P.A., Park, D.C., 2014. How does it STAC up? Revisiting the scaffolding theory of aging and cognition. Neuropsychol. Rev. 24, 355–370.

Saturnino, G.B., Antunes, A., Thielscher, A., 2015. On the importance of electrode parameters for shaping electric field patterns generated by tDCS. Neuroimage 120, 25–35.

Saturnino, G.B., Puonti, O., Nielsen, J.D., Antonenko, D., Madsen, K.H., Thielscher, A., 2019. SimNIBS 2.1: A comprehensive pipeline for individualized electric field modelling for transcranial brain stimulation. In: Makarov, S., Horner, M., Noetscher, G. (Eds.), Brain and Human Body Modeling: Computational Human Modeling at EMBC 2018. Springer International Publishing, Cham, pp. 3–25.

Schloerke, B., Crowley, J., Cook, D., Briatte, F., Marbach, M., Thoen, E., Elberg, A., Larmarange, J., 2018. GGally: extension to 'ggplot2'. R package version 1.4.0. https://CRAN.R-project.org/package=GGally.

Thomas, C., Datta, A., Woods, A., 2018. Effect of Aging on Cortical Current Flow Due to Transcranial Direct Current Stimulation: Considerations for Safety. Annu. Int. Conf. IEEE Eng. Med. Biol. Soc. 3084–3087.

Thielscher, A., Antunes, A., Saturnino, G.B., 2015. Field modeling for transcranial magnetic stimulation: a useful tool to understand the physiological effects of TMS? Conf. Proc. IEEE Eng. Med. Biol. Soc. 2015, 222–225.

Thomas, C., Datta, A., Woods, A., 2017. Effect of aging on current flow due to transcranial direct current stimulation. In: Brain Stimulation: Basic, Translational, and Clinical Research in Neuromodulation, 10, p. 469.

Verbeke, G., Molenberghs, G., 2000. Linear mixed models for longitudinal data. Springer, New York.

Wickham, H., 2016. ggplot2: Elegant Graphics for Data Analysis. Springer-Verlag, New York.

Windhoff, M., Opitz, A., Thielscher, A., 2013. Electric field calculations in brain stimulation based on finite elements: an optimized processing pipeline for the generation and usage of accurate individual head models. Hum. Brain Mapp. 34, 923–935.

Yoshida, K., 2019. tableone: Create 'Table 1' to Describe Baseline Characteristics. R package version 0.10.0. https://CRAN.R-project.org/package=tableone.